

Level statistics of disordered spin- $\frac{1}{2}$ systems and its implications for materials with localized Cooper pairs.

Emilio Cuevas¹ & Mikhail Feigel'man^{2,3} & Lev Ioffe⁴ & Marc Mezard⁵

¹Departamento de Física, Universidad de Murcia, E-30071 Murcia, Spain

²L. D. Landau Institute for Theoretical Physics, Kosygin str.2, Moscow 119334, Russia

³Moscow Institute of Physics and Technology, Moscow 141700, Russia

⁴Department of Physics and Astronomy, Rutgers University, 136 Frelinghuysen Rd., Piscataway, NJ 08854, USA

⁵CNRS, Université Paris-Sud, UMR 8626, LPTMS, Orsay Cedex, F-91405 France

Abstract

The origin of continuous energy spectra in large disordered interacting quantum systems is one of the key unsolved problems in quantum physics. While small quantum systems with discrete energy levels are noiseless and stay coherent forever in the absence of any coupling to external world, most large-scale quantum systems are able to produce thermal bath and excitation decay. This intrinsic decoherence is manifested by a broadening of energy levels which acquire a finite width. The important question is what is the driving force and the mechanism of transition(s) between two different types of many-body systems - with and without intrinsic decoherence? Here we address this question via the numerical study of energy level statistics of a system of spins- $\frac{1}{2}$ with anisotropic exchange interactions and random transverse fields. Our results present the first evidence for a well-defined quantum phase transition between domains of discrete and continuous many-body spectra in a class of random spin models. Because this model also describes the physics of the superconductor-insulator transition in disordered superconductors like InO and similar materials, our results imply the appearance of novel insulating phases in the vicinity of this transition.

Although quantum phase transitions between regimes with and without intrinsic decoherence were first discussed by Anderson in 1958 [2], their understanding is still incomplete. More recently, a number of works have studied these transitions in strongly disordered electron systems with weak repulsion [1, 17, 4] and reached the conclusion [17, 4] that a finite-temperature phase transition takes place between two regimes, “weakly insulating” and “strongly insulating”, that

are characterized by non-zero and zero conductivities respectively. In terms of the many-particle excitation spectra this result translates into the existence of an *extensive* energy threshold, with a critical excitation energy $\mathcal{E}_c \propto \mathcal{V}T_c$ that separates the discrete spectrum of excitations at $E < \mathcal{E}_c$ and continuous one at $E > \mathcal{E}_c$ for any large but finite subsystem with \mathcal{V} degrees of freedom. It also implies that the low-temperature state is free from decoherence because the lifetime of all excitations is infinite. The phase transition predicted in the work [4] was not observed yet; instead, in hopping insulators one usually observes that conductivity vanishes continuously at $T \rightarrow 0$: $\sigma(T) \sim e^{-(T^*/T)^a}$, with $a < 1$.

Different physical properties of the excitations at low and high energies in the infinite system are reflected in different statistical properties of the spectra of finite systems at $E < \mathcal{E}_c$ and at $E > \mathcal{E}_c$. Intuitively, if the eigenvectors are extended, as expected for the state where local excitations decay, they are subject to inter-level repulsion. Conversely, if the eigenvectors are localized, eigenvalues corresponding to excitations localized in different parts of the system are independent and one expects a Poisson distribution of energy levels.

Let us give a general qualitative argument in supporting this statement. Consider a small perturbation of the Hamiltonian that controls the dynamics of a generic quantum system in thermodynamic limit:

$$H \rightarrow H(1 + \dot{\phi}(t, x)) \quad (1)$$

where $\phi(t, x)$ is a generic slow function of coordinates and time. A small perturbation of this type results in the slow (adiabatic) motion of energy levels $E_n(t)$. In the absence of level repulsion, different levels cross without affecting each other, so that this motion leads only to the total phase of the wave function. Because the field $\dot{\phi}(t, x)$ (which is similar to the gravitational potential[19]) is conjugated to the energy density, the absence of response to it implies absence of the energy flux. An excitation with energy ΔE localized around point x acquires phase $\exp(-i\Delta E\phi(t, x))$ due to perturbation (1); in contrast, a delocalized excitation becomes a superposition of other excitations. Thus, the absence of the response also implies that excitations are localized and do not decay. We conclude that the absence of level repulsion implies the localization of excitations, absence of their decay and of the energy flux, i.e. formation of a strong insulator. Because level statistics can be studied for relatively small systems, this correspondence between level statistics and physical properties in thermodynamic limit provide a convenient numerical tool to predict the properties of physical systems. This strategy has been used for instance in [20].

One of the best experimental systems to test these general ideas is provided by strongly disordered superconductors (InO, TiN) in the vicinity of the disorder-induced superconductor-insulator transition [28]; for recent reviews see [16] and the introduction of the paper [11]. One advantage of these systems is that the transition can be fine-tuned by a magnetic field. In the insulating state they demonstrate purely activated behaviour $\sigma(T) \sim e^{-(T^*/T)}$, with $a = 1$. [27, 21] Far in the insulating state [28] this behaviour can be understood in terms of a single electron pseudogap [25, 24] that results from binding of

localized electrons [12, 11]. However, the persistence of an activated behavior in the vicinity of the superconductor-insulator transition (SIT) where one expects the appearance of low energy Cooper pairs requires another explanation. This was proposed in the work [18, 13] in terms of a collective mobility edge ϵ_c which separates the domain of localized excitations with energies $\omega < \epsilon_c$ from the domain of delocalized modes with $\omega > \epsilon_c$, which serves as an intrinsic thermal bath. The threshold $\epsilon_c(g)$ depends on the parameter characterizing disorder, g . It vanishes at $g = g_c$ at which superconductivity appears. At $g < g_c$ the threshold energy ϵ_c is *intensive* [18, 13] (it does not grow with the size of the system). In this regime, the density of excitations is proportional to $\exp(-\epsilon_c/T)$, leading to the activated behaviour of conductivity. At even stronger disorder, $g = g^*$, the threshold energy $\epsilon_c(g)$ diverges.

Logically there are two possibilities; the first one is that the divergence of the threshold ϵ_c at $g \rightarrow g^*$ is cut off by the system size, so that at stronger disorder ϵ_c scales with the system volume, \mathcal{V} . In this situation one expects the finite temperature transition between insulator and hard insulator predicted in [17, 4]. In the second scenario, the energy scale ϵ_c becomes really infinite at $g \rightarrow g^*$, which implies a complete localization and the absence of a thermal equilibrium at all temperatures. We will show below that both scenarios can be realized in discrete spin models depending on the detailed form of the Hamiltonian: in the models with purely local density-density interaction ϵ_c is infinite at $g < g^*$, but the addition of non-local density-density interaction terms results in the appearance of a narrow range $g_I < g < g^*$ where ϵ_c is extensive, signaling the finite temperature transition in this regime. This result raises the possibility that a finite temperature transition between strong and weak insulators might be observed in InO, TiN or similar films very close to the superconductor-insulator transition.

The theoretical work [18, 13] is based on several approximations. First, it assumes the presence of a strong pseudogap, which allows one to reduce the Hilbert space of the full electron problem to the one spanned by "pseudospin"- $\frac{1}{2}$ variables s_j^\pm, s_j^z , that describe [3] creation-annihilation and counting operators of the localized Cooper pairs. This assumption is borne out by experimental results[25]. On the theoretical side, its origin lies in the fractal structure of the wave functions near to the mobility edge of the single electron problem[12, 11]. It is further supported by direct numerical simulations of electrons with attractive interactions in a random potential[7]. The second approximation is the use of a recursion-equation technique, which becomes exact only for a special tree-like structure of a lattice completely devoid of small loops (Bethe lattice). Finally, the formalism developed in these works does not include explicitly collective excitations of high energy involving many spins. Therefore this formalism does not allow to completely settle whether the mobility edge is intensive or extensive. Note that although another prediction of our formalism, namely the anomalous broadening of the superconducting order parameter distribution in the vicinity of transition, was confirmed experimentally [25], no such data exist for insulating phase.

In the present Letter we provide a direct numerical proof of the validity of the many-body localization scenario developed in [18, 13] for a more realistic random spin lattice and taking into account the whole excitation spectrum. Our basic model contains spins $\frac{1}{2}$ that describe the absence or presence of Cooper pair on a localized single electron state. These spins are subject to random fields along the z direction and are coupled by XY interactions (2). The main physical result of our study are the phase diagrams, shown in Figs. 1 and 2, in terms of the dimensionless transverse spin coupling g and excitation energy ω (Fig.1) and temperature (Fig.2). A *size-independent (non-extensive)* threshold energy $\epsilon_c(g)$ is found in this "minimal" model, Eq.(2), for $g \in (g^*, g_c)$, while all eigenstates are localized at $g < g^*$. This implies that, for this Hamiltonian, the transition line separating the weak and hard insulators does not depend on temperature. On the other hand, we shall show that, in a model where the Hamiltonian is modified and includes additional interactions between the z components of spins, the threshold energy remains finite but *extensive* in finite systems in some range of $g < g^*$, see Fig. 2. This leads to the temperature driven transition similar to the one predicted in [17, 4].

The phase diagrams shown in Figs. 1 and 2 have another important feature: they predict a direct transition between superconductor and insulator with characteristic energy scales that go down to zero continuously on both sides of the transition, similar (but different in the important details) to the transition expected in dual theories [14, 15]. In the superconducting state this energy scale is given by the typical value of the order parameter or the transition temperature, while in the insulating states it is the value of the threshold energy $\epsilon_c(g)$, which implies the Arrhenius behavior of the resistivity at very low temperatures. These predictions are in agreement with the detailed studies of the transition driven by a magnetic field in films [26] and in Josephson junction arrays with moderate E_J/E_c [10, 22].

As discussed in details elsewhere [11, 13] a superconductor with a large pseudogap and a weak long-range Coulomb repulsion is faithfully described by the model of spins- $\frac{1}{2}$:

$$H = -W \sum_i \xi_i s_i^z - \sum_{(ij)} J_{ij}^{xy} (s_i^+ s_j^- + s_i^- s_j^+) \quad (2)$$

where points i, j belong to a random graph G with a fixed coordination number Z , $\mathbf{s}_i = \frac{1}{2}\sigma_i$ are spin- $\frac{1}{2}$ operators, $s_i^\pm = s_i^x \pm i s_i^y$, the sum $\sum_{(ij)}$ goes over all different pairs of nearest neighbors i, j on G , and all nonzero matrix elements are equal to $J_{ij}^{xy} = Wg/(Z-1)$. The random energies ξ_j are uncorrelated at different sites and chosen from the box distribution $Q(\xi) = \frac{1}{2}\theta(1-|\xi|)$, corresponding to bandwidth W .

Eigenstates of the Hamiltonian (2) are vectors in the 2^N -dimensional Fock space (N is the total number of sites of G). As discussed above, the transition between decoherent and coherent states can be deduced from the change in the statistics of the exact eigen-energies E_i of the Hamiltonian. To identify the energy level statistics, we study the dimensionless parameter $r_n \in [0, 1]$ defined

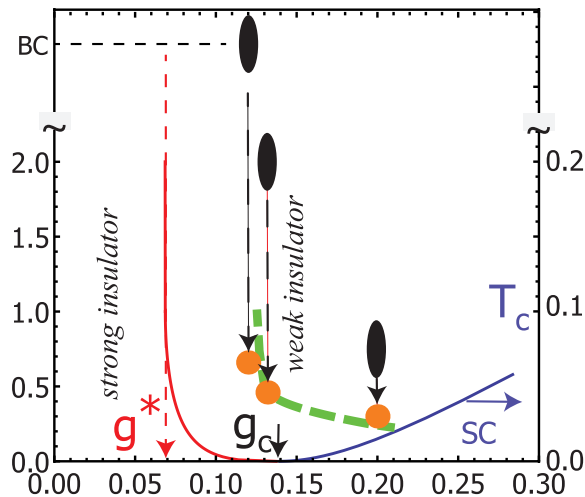


Fig. 1: Phase diagram of a strongly disordered superconductor with a large pseudogap as a function of interaction constant g . The full lines show the predictions of the analytical theory of the model (2) for the critical temperature (right vertical axis) and the threshold energy, ϵ , (left axis) of spin flip excitations in infinite random graph with $Z = 3$ neighbors. The vertical ovals show the values of the critical coupling constant that correspond to a transition between different types of spectra for different energies E in the finite random graph model of a small size ($N = 16 - 20$) as determined by direct numerical simulations. The uppermost oval shows the transition at the many-body band center (corresponding to $E \gg 1$) that sets a lower bound for the critical $g(E)$. The thick dashed line shows the position of the spectral threshold for single-spin excitations with energy ϵ adjusted by finite-size effects, as explained in the main text and in the Supplement A.2. The small circles show the typical energy of the single-spin excitations, $\epsilon(E)$, that give the main contribution to the many body excitations studied in direct numerical simulations. The good agreement between their position and expectations (dashed line) confirms the validity of the cavity method [18, 13] that is used to obtain the results in large systems. The very small change in the critical value of the coupling constant between excitations at energy $E \approx 2.0$ and the band center implies that all excitations, at high and low energies, become localized when $g < g^*$.

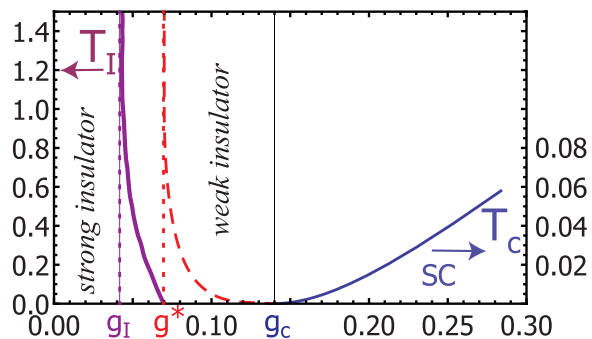


Fig. 2: Phase diagram in the temperature - coupling constant plane for the model (4) with $Z = 3$ ($K = 2$), obtained from the solution of cavity equations. The strength of the $s^z s^z$ interaction is $J^z = 0.1$. This interaction leads to a qualitatively new phenomenon, the appearance of a finite temperature transition between weak and strong insulators. In the weak insulator, excitations at sufficiently high energies can decay even at zero temperature. A non-zero temperature results in non-zero relaxation of all excitations, even the ones of lowest energy. In contrast, in the strong insulator, no excitation with intensive energy can decay. As the interaction constant is decreased, the temperature separating these phases goes to infinity at $g = g_I$. At smaller coupling $g < g_I$, all excitations, even those with *extensive* energy remain localized. The value of $g_I \approx 0.042$ is approximately equal to $0.30g_c$. The ratio $g_I/g_c = 0.3$ is in good agreement with the results of the direct diagonalization on small graphs, as can be seen from the critical values of J_c^{XY} found in Fig.3: 0.02 for the middle of the band and 0.74 for the low energies.

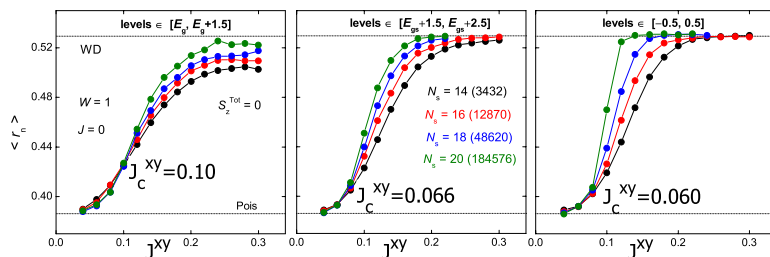


Fig. 3: The energy-level statistics is characterized by the average $\langle r_n \rangle$ that distinguishes Wigner-Dyson and Poisson distributions (values of $\langle r_n \rangle$ corresponding to these distributions are shown by dashed lines). The left panel shows the statistics of the low-energy excitations in the energy interval $(E_{gs}, E_{gs} + 1.5)$ as a function of the transverse interaction constant, J^{xy} , for the $Z = 3$ random graph with bandwidth $W = 1$. The middle panel shows similar results for intermediate energies, and the right panel corresponds to high energies, close to the center of the many-body spectrum.

as

$$r_n = \min(\delta_n, \delta_{n-1}) / \max(\delta_n, \delta_{n-1}) \quad (3)$$

where $\delta_n = E_n - E_{n-1}$ and E_n is the n -th energy level. The average value $r = \langle r_n \rangle$ is equal to 0.38 for Poisson level statistics, and to 0.53 for Wigner-Dyson statistics. In the limit of infinite systems one expects a sharp transition between these two values as a function of g , or of the energy. In a finite system the parameter r increases smoothly, but the curve $r(g)$ is expected to become steeper as the size is increased.

The appearance of a unique crossing point of these curves for different sizes N implies a well-defined phase transition in the limit of infinite-size systems. This is seen in the exact diagonalization of the Hamiltonian (2) with $Z = 3$, shown in Fig. 3. Apart from the persistence of the transition for small system sizes, these data also show that the critical value of J^{xy} changes very little as the energy is increased to the center of the band. This proves that high energy states in this model become localized together with the low energy ones, in more physical terms it implies that no new decay channels appear at high energies. The absence of new decay processes at high energies is the physical reason why in this model one does not get the intermediate phase with *extensive* energy threshold. Also, these data show that the transition happens at a value $r_n(g)$ that is close to its value 0.38 expected for Poisson statistics. This is due to a large distribution of relaxation rates in these systems[13] that implies that in case of small systems many realizations of the random energies give localized states, while delocalization only happens with a small probability as we explain in a more detail below.

In order to compare quantitatively the results of the direct diagonalization shown in Fig. 3 with the predictions of the theory [13] we need to take into

account the finite size effects. They are very significant for the sizes (number of spins $N \leq 20$) available for direct diagonalization, for two reasons. First, in a finite system the crossover from Poisson to Wigner-Dyson statistics is expected to occur when the level spacing $\delta(E) = \nu^{-1}(E)$ becomes approximately equal to the level width $\Gamma(E)$ expected theoretically. The latter quickly becomes exponentially small[13] when the transition in the infinite system is approached, so that the condition $\delta(E) = \Gamma(E)$ in a finite (not very large) system is satisfied far away from the transition in the infinite system. Second, the level widths fluctuate wildly from one finite system to another in small systems. Because the infinite system can be viewed as being composed of small ones, each of these parts having many neighbors, even a small probability to find a delocalized (finite width) level in a small system is sufficient for delocalization in the infinite system. This makes the typical decay rate in the infinite system much larger than the one in a collection of small ones. Both effects combine to push up the apparent critical value of g by roughly a factor of two. Finally, for the quantitative comparison, we need to take into account that the critical point condition $\delta(E) = \Gamma(E)$ applies to the level spacing and total level width in the many body systems, whereas the analytical theory [13] gives the level width of individual spin flips. The typical level at energies $E \gtrsim W$ consists of a few spin flips, which decay rates add to the total width $\Gamma(E)$. The main contribution to the typical level at energy $E \gtrsim W$ comes from single-spin excitations in a relatively narrow energy window $\epsilon(E) \approx \sqrt{EW/N}$, see Supplement A.1. This allows us to interpret the crossing point in exact diagonalization as the delocalization of individual spin flips as shown in Fig. 1. We present the details in the Supplement A.2.

These results are consistent with the recent findings of paper [8] which studied a model similar to our (2) but with identical $s_i^+ s_j^-$ -couplings between all pairs of spins, allowing exact integrability of the Hamiltonian. The conclusion reached in this work is that many-body delocalized state disappears in exactly integrable case but reappears when variations of couplings between spins are allowed that destroys integrability. In the latter case one expects a sharp transition between localized and delocalized regimes similar to the one found in model (2).

We now discuss the generality of the conclusions reached above. The absence of an intermediate phase with extensive energy threshold can be traced back to the irrelevance of interactions between individual spin flips. One can thus expect new physics to appear if such interaction is introduced. The simplest and most physical model that has an additional interaction between spin flips includes an additional "longitudinal" spin-spin interaction:

$$\tilde{H} = -W \sum_i \xi_i s_i^z - \sum_{(ij)} J^z s_i^z s_j^z - \sum_{(ij)} J_{ij}^{xy} (s_i^+ s_j^- + s_i^- s_j^+) \quad (4)$$

that can be viewed as due to the long range part of Coulomb interaction ($J^z < 0$) or to phonon mediated attraction between electrons ($J^z > 0$) [11]. As will be clear below, the results do not depend on the sign of $J^z \ll W$. The first two

terms in the Hamiltonian (4) describe a classical Ising magnet in a random field. We shall be interested in its disordered phase which is realized when the longitudinal interaction is small, $J^z \ll W$. In this case the classical eigenstates of this magnet coincide with that of independent spins, with energies that are weakly modified by the interaction. In the absence of transverse interactions the excitations of this magnet are individual spin flips with energies $\epsilon_i = W\xi_i + J^z \sum_{j(i)} s_j^z$. In the ground state the direction of almost all spins is determined by the sign of the random field, so the presence of a small J^z affects weakly the density of states of these low-energy excitations and their decay due to transverse interaction. Thus we expect that the low-energy properties of the spectrum remain similar to the model with zero J^z . The situation is very different at high energies when the decay of a given spin occurs against the background of different spin configurations. Physically, a spin excitation at energy ϵ has a much larger chance to propagate through a given site if the energy of the spin flip at this site is close to ϵ . The energy of a spin flip is distributed with the probability density $Q(\xi)$, where $\xi = \epsilon/W$, if all surrounding spins are locked into a fixed configuration. In contrast, at extensive energies, the surrounding spins acquire many different configurations. This increases the probability that a given site is in resonance with the excitation. This effect can be also described as being due to the interaction between individual spin flip processes that allow new channels for the decay of these excitations. This should result in the large suppression of the critical value of the interaction constant at high energies.

The exact diagonalization of the Hamiltonian on a $Z = 3$ random graph with $J^z = 0.1$ confirms these expectations (Figure 4). In presence J^z , the value $g_c(0)$ is shifted slightly downwards for low energies ($J_c = 0.10 \rightarrow 0.074$). The shift becomes substantial for medium energies ($J_c = 0.066 \rightarrow 0.04$) and very large for energies close to the band center: $J_c = 0.06 \rightarrow 0.02$. A slight shift of the critical value of the interaction constant at low and medium energies is probably due to the fact that at these energies a typical excited state contains more than one spin-flip excitation. As explained above, the interaction between these excitations leads to delocalization.

The solution of cavity equations, similar to those solved in [13] (see Supplement A.3) confirms the appearance of the extensive threshold for $J^z \neq 0$ and gives the dependence of the transition temperature $T_I(g)$ on the coupling constant g that we show in Fig. 2 for $J^z = 0.1$. At $g < g^*$ and $T < T_I(g)$ all excitations with intensive energies are localized, no transport of any sort is possible. In contrast, at higher temperatures $T > T_I(g)$ all excitations, even those with low energies, acquire a non-zero width. At $g > g^*$ and zero temperature, the excitations with low energy are localized while high energy excitations decay. This latter distinction is smeared at any non-zero temperature because the presence of even a small density of mobile high energy excitations leads to a slow decay of even lowest energy ones.

The main conclusion of our work is the existence of two different insulating phases and a prediction of the finite temperature transition between a weak insulator characterized by an activated transport and a strong one in which no transport occurs. Experimentally, the second transition might be detected by

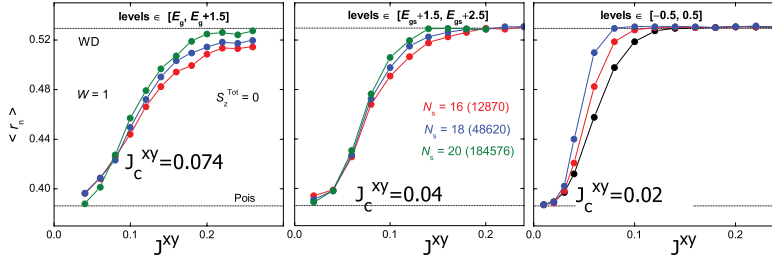


Fig. 4: Level statistics, characterized by the parameter $\langle r_n \rangle$ in the presence of weak longitudinal spin coupling J for low energy levels (left panel), intermediate energies (middle panel) and center of the many body band (right panel). Even a small coupling $J^z = 0.1$ has a significant effect, it shifts the transition to much smaller values of the transverse coupling g .

the onset of an anomalously slow thermalization[9]. These results are obtained within a lattice spin- $\frac{1}{2}$ model which serves as a good approximation to the description of the superconductor-insulator transition in a number of materials. We believe that it might be possible to observe this transition in insulating films in a close proximity to the superconducting transition. Due to a finite value of the pseudogap in a realistic systems, a temperature-driven transition between weak and strong insulating phases will be seen as a sharp crossover in resistivity curves $R(T)$, with a rapid growth of the apparent activation energy $d \ln R(T)/d(1/T)$ as T decreases. Some preliminary experimental evidence for this behaviour in TiN was reported in [5], it was also observed in InO_x [23].

EC and MF thank the FEDER and Spanish DGI for financial support through project FIS 2010-16430. MF acknowledges support through RFBR grant 10-02-00554 and RAS program "Quantum physics of condensed matter", LI was supported by ARO W911NF-09-1-0395, DARPA HR0011-09-1- 0009 and NIRT ECS-0608842.

A Supplementary online material

A.1 Density of states

For the quantitative analysis of the numerical results we need the energy dependence of the total density of states $\nu(E)$ of the Hamiltonian (2). As we explain in detail below, at low energies $E \leq N$ it is given by the formula first found by H. Bethe [6] for heavy nuclei:

$$\nu(E) = CN \exp(\alpha \sqrt{EN}) \quad (5)$$

where $C \sim 1$ and $\alpha \sim 1$ are functions which depend only weakly on g . This equation and the discussion below assume that the band width is chosen as $W = 1$. The numerical data presented in Fig. 5 show that the density of many

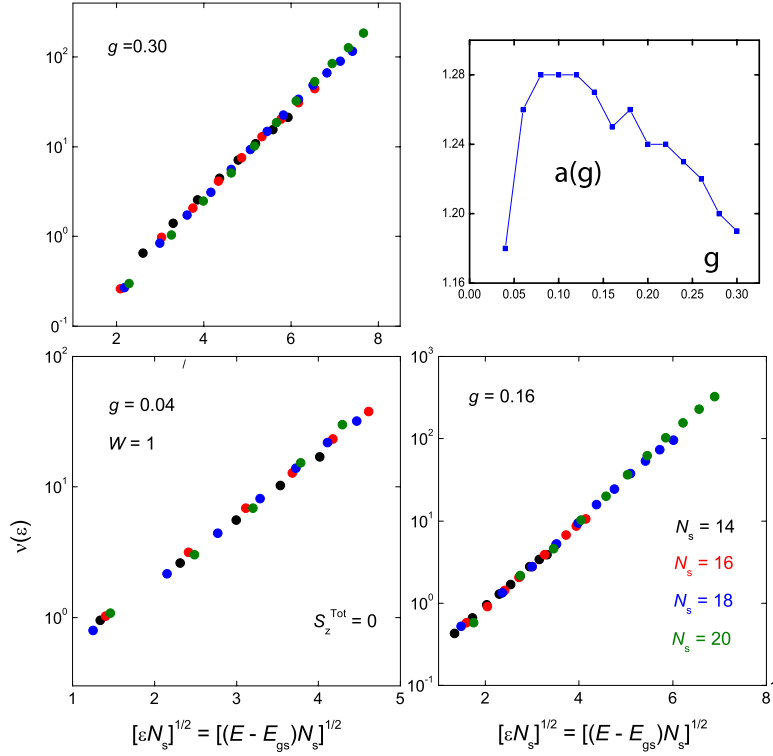


Fig. 5: Density of states of the Hamiltonian (2) obtained for $g = 0.04$, $g = 0.16$ and $g = 0.30$, as indicated on the panels. The coefficient $a(g)$ is determined by the slope of the straight lines that provide the best fit to the data points. The upper right panel shows the $a(g)$ dependence. It displays a maximum for g close to the critical point g_c .

body levels of Hamiltonian (2) are indeed given by Eq.(5) for all values of g , with a weakly g -dependent coefficient $a(g)$. Because the functional form of $\nu(E)$ is g -independent, one can understand its origin by considering the simple problem of non-interacting spins, defined by the first term of (2).

In this approximation the excitation energy is $E = \sum_{i=1,N} \eta_i \sigma_i$ where σ_i are equal to 0 or 1, and $\eta_i \in [0, 1]$ are quenched random parameters. Let us denote by $\nu(E)$ the typical density of states. Its Laplace transform, for one given instance (i.e. one given realization of η_i) is

$$\tilde{\nu}(s) = \sum_{s_i \in \{0,1\}} \exp\left(-\sum \eta_i \sigma_i s\right) = \prod_i (1 + e^{-s\eta_i}) . \quad (6)$$

For a large system, this density of states self-averages, in the sense that $\log \nu$

goes to a well defined limit:

$$\log \tilde{\nu}(s) = N \int_0^1 d\eta \log(1 + e^{-s\eta}) . \quad (7)$$

In order to reconstruct the typical density of states using the inverse Laplace transform, we must find the maximum over s of $E s + N \int_0^1 d\eta \log(1 + e^{-s\eta})$. The value of s at which this expression is maximal satisfies the equation

$$\frac{E}{N} = \int_0^1 d\eta \frac{\eta e^{-\tilde{s}\eta}}{1 + e^{-\tilde{s}\eta}} \quad (8)$$

leading to

$$\nu(E) \approx \frac{1}{\sqrt{E}} \exp \left\{ N_s \int_0^1 d\eta \ln [1 + e^{-\tilde{s}\eta}] + E \tilde{s} \right\} \quad (9)$$

In the limit of small E/N the maximum is found at large s , so that

$$\frac{E}{N} \simeq \frac{1}{\tilde{s}^2} \int_0^\infty dx \frac{x e^{-x}}{1 + e^{-x}} = \frac{c}{\tilde{s}^2} \quad (10)$$

where $c = \frac{\pi^2}{12}$. Altogether this shows that the density of states grows as $e^{\alpha\sqrt{N_s E}}$, where

$$\alpha = 2\sqrt{c} = \frac{\pi}{\sqrt{3}} \approx 1.8 \quad (11)$$

For realistic N , however, the minimum is somewhat different as can be seen from the Figure 6 in which we show the full expression (9) for $N = 18$ and its fit to the square root dependence.

In comparison, the direct numerical simulation of 100 realizations for $N = 18$ system shows a similar behavior with slightly smaller coefficient $a = 1.25 - 1.35$. The asymptotic (5) does not change if we restrict the states to the sector $S^z = 0$ computed numerically, see Figure 6 where we show the results restricted to this sector.

In the energy range $1 \leq E \leq N$, the most probable number $n(E)$ of single-spin excitations whose energies sum up to E , is $n(E) \approx \sqrt{EN}$. Typical single-spin excitation energies are $\epsilon(E) = \sqrt{E/N}$.

At higher energies, density of states reaches its maximum at $E = E_0 \sim N$, with $\ln \nu(E_0) \sim N$, where E_0 corresponds to the center of the many-body band. One can relate extensive energy $E = \epsilon N$ of the spin system and its temperature T , assuming internal equilibrium:

$$T = \left(\frac{d \ln \nu(E)}{dE} \right)^{-1} = \frac{2}{\alpha} \epsilon(E) \quad \text{for } E \ll N \quad (12)$$

Equation (12) shows that typical single-spin excitation energy grows with temperature as $\epsilon = \alpha T/2$. Note that $T(E)$ diverges as energy approaches band center, $T^{-1}(E_0) = 0$.

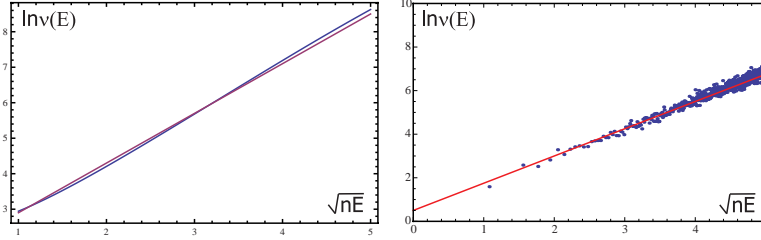


Fig. 6: Density of states and its approximations. The left panel shows the density of states given by the full analytical formula (9) and its approximation by the simplified square root dependence $\ln \nu = a\sqrt{NE} + b$ for $N = 18$ with $a = 1.4$ and $b = 1.5$. The right panel shows the direct numerical simulation of 100 realization for the system of 18 spins in sector $S_z = 0$ and its fit to a $\ln \nu = a\sqrt{nE} + b$ dependence, with $a = 1.25$, $b = 0.5$.

A.2 Finite-size effect upon the transition line

In a finite system the crossover from the Poisson to Wigner-Dyson statistics is expected to occur when the states become delocalized. Delocalization implies that the width of the level determined self-consistently in the cavity approach [13] is of the order of the level spacing. A number of finite size effects make the direct comparison between the analytical results for infinite systems[13] and numerical results reported here non-trivial. First, the width, $\Gamma(E)$, of the level is expected to become exponentially small as the energy threshold is approached:

$$\Gamma(\epsilon) \sim e^{-\frac{\omega_1}{\epsilon - \epsilon_c(g)}}$$

Furthermore, the coefficient, ω_1 in this equation is much larger (see Ref. [13]) than ϵ_c , so the decay rate becomes very small even relatively far from the transition line. In a finite system with a not-so-small level spacing, this leads to a very significant shift of the apparent critical energy due to finite size effects. Second, the width of the levels fluctuate strongly from one graph realization to another, see insert in Fig. 7. The large peak at small values of Γ shows that in many realizations the level width is essentially zero. The change in the statistics observed in small systems is due to a relatively small number of graphs with significant Γ . This explains why the crossover is always observed at a value of r_n that is close to the one of Poisson statistics. In order to compute the critical value of the coupling constant expected in finite systems we evaluated the probability, $P(\Gamma_0)$ to find the level width $\Gamma > \Gamma_0$ obtained by the solution of cavity equations for the systems of this size. The result is shown in Fig. 7 for a typical value of ϵ and Γ_0 . The crossing point observed by direct numerical diagonalization is expected to happen when the probability $P(\Gamma_0 = \delta(E))$ becomes non-zero. To avoid the problem with numerical errors, we used the condition $P(\Gamma_0 = \delta(E)) > \delta_0$ with $\delta_0 = 0.004 - 0.02$ and checked that the results are not sensitive to the specific value of δ_0 in this interval. Using this condition we take

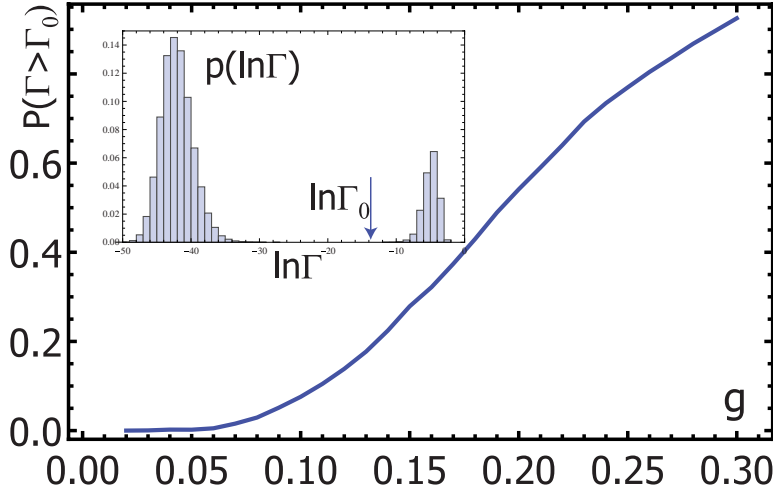


Fig. 7: The solution of cavity equations in finite random graphs gives a widely distributed width Γ of single spin flip excitations. The insert shows the probability distribution of $\Gamma(\omega)$ for $\omega = 0.35W$ in a random graph with $N = 20$ spins and a coupling constant $g = 0.10$. The right-hand peak in this distribution corresponds to all graphs in which a significant $\Gamma(\omega)$ is spontaneously formed. The main panel shows the weight of the graphs in which a significant $\Gamma(\omega)$ (defined as $\ln \Gamma > \ln \Gamma_0$) is formed as a function of the interaction constant g . The resulting value is only weakly sensitive to the value of the cutoff Γ_0 for most ω and g . This allows us to determine the apparent critical value of the interaction constant $g(\omega)$ for the finite systems. The results are shown in Fig.1 as a dashed line.

into account both finite size effects and compute the finite-size corrections to the infinite-system $\epsilon_c(g)$ predicted analytically. The final result for the apparent transition for small sizes is shown in Fig. 1 by the green line, it is shifted with respect to the infinite-size $\epsilon_c(g)$ shown by red line by a factor of two.

Finally, when comparing the predictions of the cavity equations with the results of the exact diagonalization, we have to take into account that high energy levels of the whole system correspond to many spin flips: the resulting decay rate is the sum of the decay rates of the individual flips. Because of the weak (logarithmic) dependence of the probability $P(\Gamma_0)$ on Γ_0 this fact has a very weak effect on the expected transition. Because of the fast (exponential) dependence of the density of states on the energy, the typical spin flip contributing to the high energy level has a well defined energy given by the saddle point solution of section A.1: $\epsilon(E) \sim \sqrt{EW/N}$. This allows us to map the energies, E , studied in the numerical diagonalization to a typical energy of a single flip, $\epsilon(E)$, and to compare the results of the numerical diagonalization and solution of cavity equations as shown in Fig. 1.

A.3 $S_z - S_z$ coupling and finite- T phase transition

In the previous papers [18, 13] we derived a recursion relation for the intrinsic level widths Γ_i of single-spin-flip excitations, assuming a local Bethe lattice structure of the lattice:

$$\Gamma_i = (J^{xy})^2 \sum_{k(i)} \frac{\Gamma_k}{(\omega - W|\xi_k|)^2 + \Gamma_k^2} \quad (13)$$

where $k(i)$ are the $K = Z - 1$ neighbours of i in the cavity graph. The same recursions can be used for a random graph model studied in the present paper, upon neglecting the contributions of closed loops (loops are totally absent on the infinite Bethe lattice whereas they are present with parametrically low density $\sim 1/\ln N$ on a random graph with N sites). The condition of stationarity of the distribution function $P(\Gamma)$ generated by the mapping (13) leads to the solution for typical $\Gamma_{typ}(\omega)$ found in Ref. [13].

In presence of $s_i^z s_j^z$ coupling the recursion equations (13) should be modified. At nonzero temperature $T = \beta^{-1}$ it contains the sum over neighboring spin configurations with their thermal weights:

$$\Gamma_i = (J^{xy})^2 \sum_{k(i)} \sum_{s_{n(k)}^z} \frac{e^{\xi_n s_{n(k)}^z / T}}{Z_k} \frac{\Gamma_k}{(\omega - \epsilon_k)^2 + \Gamma_k^2} \quad (14)$$

where the internal summation over $s_{n(k)}^z$ includes all configurations of spin variables connected to the spin s_k by $z - z$ links, $Z_k = \sum_{s_{n(k)}} e^{\beta \xi_n s_{n(k)}^z}$ are the corresponding local partition functions, and $\epsilon_k = W|\xi_k| + J^z \sum_{n(k)} s_n^z$.

The largest contribution to the sum (13) comes from the site k characterized by ξ_k that is closest to ω . The same holds for the sum (14), but in addition in this sum the value of ϵ_k varies depending on the surrounding spins. This increases the probability to find a resonance. To evaluate the importance of this effect we consider explicitly the case of $Z = 3$ (corresponding to the random graphs diagonalized in this paper) and the energy at center of the band, $\omega = W/2$. The critical value of the coupling constant in this case is determined by the condition $\overline{\ln \Xi} = 0$ in the limit of the large system size. Here

$$\Xi = \sum_{j\{i\}} \prod_j \left(\frac{g}{K}\right)^2 \frac{1}{Z_j} \left\{ \frac{e^{-\beta(\xi_{j1} + \xi_{j2})}}{(\delta\xi_j + 2\gamma)^2} + \frac{2 \cosh \beta(\xi_{j1} - \xi_{j2})}{\delta\xi_j^2} + \frac{e^{\beta(\xi_{j1} + \xi_{j2})}}{(\delta\xi_j - 2\gamma)^2} \right\} \quad (15)$$

is the relaxation rate induced deep in the system center by the infinitesimally small couplings at the boundary, $Z_j = 4 \cosh \beta \xi_{j1} \cosh \beta \xi_{j2}$, $\gamma = J^z / W$, $\beta = 2T/W$ and $\delta\xi_j = \xi_j - \omega$. Performing the same steps as in Ref. [13] we average over the distribution of ξ using the replica method and we get the condition for

the critical value of $g(T)$:

$$g = K \exp \left[-\frac{1}{2} \min_x f(x) \right]$$

$$f = \frac{1}{x} \ln \left\{ K \int d\xi d\xi_1 d\xi_2 \left[\frac{1}{Z(\xi_1, \xi_2)} \left(\frac{e^{-\beta(\xi_1 + \xi_2)}}{(\delta\xi + \gamma)^2} + \frac{2 \cosh \beta(\xi_1 - \xi_2)}{\delta\xi^2} + \frac{e^{\beta(\xi_1 + \xi_2)}}{(\delta\xi - \gamma)^2} \right) \right]^x \right\}$$

The inversion of the obtained function $g(T)$ provides the $T_I(g)$ dependence shown in Fig.2 by the thick violet line.

References

- [1] Boris L. Altshuler, Yuval Gefen, Alex Kamenev, and Leonid S. Levitov. Quasiparticle lifetime in a finite system: A nonperturbative approach. *Phys. Rev. Lett.*, 78(14):2803–2806, Apr 1997.
- [2] P. W. Anderson. Absence of diffusion in certain random lattices. *Phys. Rev.*, 109(5):1492–1505, Mar 1958.
- [3] P.W. Anderson. Theory of dirty superconductors. *Journal of Physics and Chemistry of Solids*, 11(1-2):26 – 30, 1959.
- [4] D.M. Basko, I.L. Aleiner, and B.L. Altshuler. Metal-insulator transition in a weakly interacting many-electron system with localized single-particle states. *Annals of Physics*, 321(5):1126 – 205, 2006.
- [5] T.I. Baturina, A Yu. Mironov, V. M. Vinokur, M. R. Baklanov, and C. Strunk. Hyperactivated resistance in titanium nitride films on the insulating side of the disorder-driven superconductor-insulator transition. *JETP Lett.*, 88:752, 2008.
- [6] H. A. Bethe. An attempt to calculate the number of energy levels of a heavy nucleus. *Phys. Rev.*, 50:336–, 1936.
- [7] Karim Bouadim, Yen Lee Loh, Mohit Randeria, and Nandini Trivedi. Single and two-particle energy gaps across the disorder-driven superconductor-insulator transition. *cond-mat arXiv:1011.3275*, 2010.
- [8] F. Buccheri, A. De Luca, and A. Scardicchio. On the structure of typical states of a disordered richardson model and many-body localization. *arXiv:1103.3431*, Mar 2011.
- [9] Elena Canovi, Davide Rossini, Rosario Fazio, Giuseppe E. Santoro, and Alessandro Silva. Quantum quenches, thermalization, and many-body localization. *Phys. Rev. B*, 83:094431, Mar 2011.
- [10] R. Fazio and H. van der Zant. Quantum phase transitions and vortex dynamics in superconducting networks. *Physics Reports-review Section of Physics Letters*, 355(4):235–334, December 2001.

-
- [11] M. V. Feigel'man, L. B. Ioffe, V. E. Kravtsov, and E. Cuevas. Fractal superconductivity near localization threshold. *Annals of Physics*, 325(7, Sp. Iss. SI):1390–1478, July 2010.
- [12] M. V. Feigel'man, L. B. Ioffe, V. E. Kravtsov, and E. A. Yuzbashyan. Eigenfunction fractality and pseudogap state near the superconductor-insulator transition. *Phys. Rev. Lett.*, 98(2):027001, Jan 2007.
- [13] M. V. Feigel'man, L. B. Ioffe, and M. Mézard. Superconductor-insulator transition and energy localization. *Phys. Rev. B*, 82(18):184534, Nov 2010.
- [14] Matthew P. A. Fisher. Quantum phase transitions in disordered two-dimensional superconductors. *Phys. Rev. Lett.*, 65:923–926, Aug 1990.
- [15] Matthew P. A. Fisher, G. Grinstein, and S. M. Girvin. Presence of quantum diffusion in two dimensions: Universal resistance at the superconductor-insulator transition. *Phys. Rev. Lett.*, 64:587–590, Jan 1990.
- [16] V. F. Gantmakher and V. T. Dolgoplov. Superconductor - insulator quantum phase transition. *Physics - Uspekhi*, 53:3, 2010.
- [17] I. V. Gornyi, A. D. Mirlin, and D. G. Polyakov. Interacting electrons in disordered wires: Anderson localization and low- t transport. *Phys. Rev. Lett.*, 95(20):206603, Nov 2005.
- [18] L. B. Ioffe and Marc Mézard. Disorder-driven quantum phase transitions in superconductors and magnets. *Phys. Rev. Lett.*, 105(3):037001, Jul 2010.
- [19] J. M. Luttinger. Theory of thermal transport coefficients. *Phys. Rev.*, 135(6A):A1505–A1514, Sep 1964.
- [20] Vadim Oganesyan and David A. Huse. Localization of interacting fermions at high temperature. *Phys. Rev. B*, 75(15):155111, Apr 2007.
- [21] M. Ovadia, B. Sacépé, and D. Shahar. Electron-phonon decoupling in disordered insulators. *Phys. Rev. Lett.*, 102(17):176802, Apr 2009.
- [22] J. Paramanandam, M.T. Bell, , L.B. Ioffe, and M.E. Gershenson. Magnetic field driven quantum transitions in josephson arrays. *to be published*, 2011.
- [23] B. Sacepe. *Private communication*, 2011.
- [24] B. Sacepe, C. Chapelier, T.I. Baturina, V.M. Vinokur, M.R. Baklanov, and M. Sanquer. Pseudogap in a thin film of a conventional superconductor. *Nature Communications*, 1:140, 2010.
- [25] B. Sacepe, T. Dubouchet, C. Chapelier, M. Sanquer, M. Ovadia, D. Shahar, M. Feigel'man, and L. Ioffe. Localization of preformed cooper pairs in disordered superconductors. *Nature Physics*, 7(3):239 – 44, 2011.

-
- [26] G. Sambandamurthy, L. W. Engel, A. Johansson, E. Peled, and D. Shahar. Experimental evidence for a collective insulating state in two-dimensional superconductors. *Phys. Rev. Lett.*, 94(1):017003, Jan 2005.
- [27] G. Sambandamurthy, L. W. Engel, A. Johansson, and D. Shahar. Superconductivity-related insulating behavior. *Phys. Rev. Lett.*, 92(10):107005, Mar 2004.
- [28] D. Shahar and Z. Ovadyahu. Superconductivity near the mobility edge. *Phys. Rev. B*, 46(17):10917–10922, Nov 1992.